Neuron, Vol. 46, 541–554, May 19, 2005, Copyright ©2005 by Elsevier Inc. DOI 10.1016/j.neuron.2005.04.008

Presenilin-Dependent Transcriptional Control of the Aβ-Degrading Enzyme Neprilysin by Intracellular Domains of βAPP and APLP

Raphaëlle Pardossi-Piquard,[1] Agnès Petit,[1] Toshitaka Kawarai,[2] Claire Sunyach,[1] Cristine Alves da Costa,[1] Bruno Vincent,[1] Sabine Ring,[3] Luciano D'Adamio,[4,5] Jie Shen,[6] Ulrike Müller,[3] Peter St. George Hyslop,[2] and Frédéric Checler[1,*]

[1]Institut de Pharmacologie Moléculaire et Cellulaire
Centre National de la Recherche Scientifique
UMR6097 CNRS/UNSA
Valbonne 06560
France

[2]Centre for Research in Neurodegenerative Diseases
Department of Medicine
University of Toronto and University Health Network
Toronto Western Hospital Research Institute
6 Queen's Park Crescent
Toronto, Ontario M5S 3H2
Canada

[3]Institute for Pharmacy and Molecular Biotechnology
University of Heidelberg
69120 Heidelberg
Germany

[4]Albert Einstein College of Medicine
New York, New York

[5]Dipartimento di Biochimica e Biotecnologie Mediche
Universita' Degli Studi di Napoli Federico II
Napoli
Italy

[6]Center for Neurologic Diseases
Harvard Medical School
Boston, Massachusetts

Summary

Amyloid β-peptide (Aβ), which plays a central role in Alzheimer's disease, is generated by presenilin-dependent γ-secretase cleavage of β-amyloid precursor protein (βAPP). We report that the presenilins (PS1 and PS2) also regulate Aβ degradation. Presenilin-deficient cells fail to degrade Aβ and have drastic reductions in the transcription, expression, and activity of neprilysin, a key Aβ-degrading enzyme. Neprilysin activity and expression are also lowered by γ-secretase inhibitors and by PS1/PS2 deficiency in mouse brain. Neprilysin activity is restored by transient expression of PS1 or PS2 and by expression of the amyloid intracellular domain (AICD), which is cogenerated with Aβ, during γ-secretase cleavage of βAPP. Neprilysin gene promoters are transactivated by AICDs from APP-like proteins (APP, APLP1, and APLP2), but not by Aβ or by the γ-secretase cleavage products of Notch, N- or E- cadherins. The presenilin-dependent regulation of neprilysin, mediated by AICDs, provides a physiological means to modulate Aβ levels with varying levels of γ-secretase activity.

*Correspondence: checler@ipmc.cnrs.fr

Introduction

One of the two main histopathological hallmarks in Alzheimer's disease (AD) is the senile plaque, an extracellular protein deposit composed in part by fibrillar aggregates of amyloid β-peptides (Aβ) (Haass and Selkoe, 1993). Aβ is a 40–42 amino acid peptide that is generated from the β-Amyloid Precursor Protein (βAPP) by two sequential cleavages. The first of these cleavages occurs in the extracellular domain and is mediated by a membrane-bound aspartyl protease termed β-secretase (Vassar and Citron, 2000). The second set of cleavages occurs at residues 40–42 (termed γ-site) and at residues 48–52 (termed ε-site) within the transmembrane domain of the βAPP stub generated by β-secretase. The γ-site cleavage generates Aβ, while the concurrent ε-site cleavage generates a cytosolic stub referred to as ICD (Passer et al., 2000) or AICD (βAPP IntraCellular Domain). The exact role of AICD remains unclear.

Both the γ- and the ε-site cleavages are mediated by presenilin (PS)-independent and dependent proteases (De Strooper et al., 1998; Armogida et al., 2001). The presenilin-dependent γ-secretase and ε-site proteolytic activities (which are often generically collectively termed γ-secretase) are dependent upon a multimeric complex of at least four different membrane proteins including Presenilin 1(PS1) or Presenilin 2 (PS2), nicastrin, Aph-1, and Pen-2 (Yu et al., 2000; Francis et al., 2002). In these complexes, the presenilins have been proposed as a novel type of transmembrane aspartyl protease bearing the catalytic core of the γ-secretase (Wolfe et al., 1999).

This novel type of intramembranous proteolysis apparently governs the function of βAPP and several Type I transmembrane proteins including Notch, cadherins, ErbB-4, CD44, or $p75^{NTR}$. Many of these proteins are involved in a variety of vital cellular functions such as intracellular signaling in development and adulthood, cell adhesion, cell growth and proliferation, and kinase activities (for review see Sisodia and St. George-Hyslop, 2002; Pollack and Lewis, 2005). Thus, γ-secretase cleavage of Notch releases an intracellular fragment called NICD (Notch IntraCellular Domain), which acts as a transcription factor mediating signal transduction in the Notch-Delta pathway, a critical intercellular signaling mechanism, during both embryonic development and adulthood (Kopan et al., 1996; Shen et al., 1997; De Strooper et al., 1998; Kopan and Goate, 2000).

Under normal conditions, Aβ occurs as a soluble fragment, the concentration of which is normally tightly controlled below the threshold for its self-aggregation into β sheet fibrils (Burdick et al., 1992). Aβ is actively degraded by several enzymes including neprilysin (NEP), insulin-degrading enzyme (IDE), and endothelin-converting enzyme (ECE) (Carson and Turner, 2002). Although these Aβ-degrading enzymes have been well characterized, very little is known about the regulatory mechanisms that govern their expression and/or activity. Nevertheless, under normal physiological circumstances, the balance between the rates of production

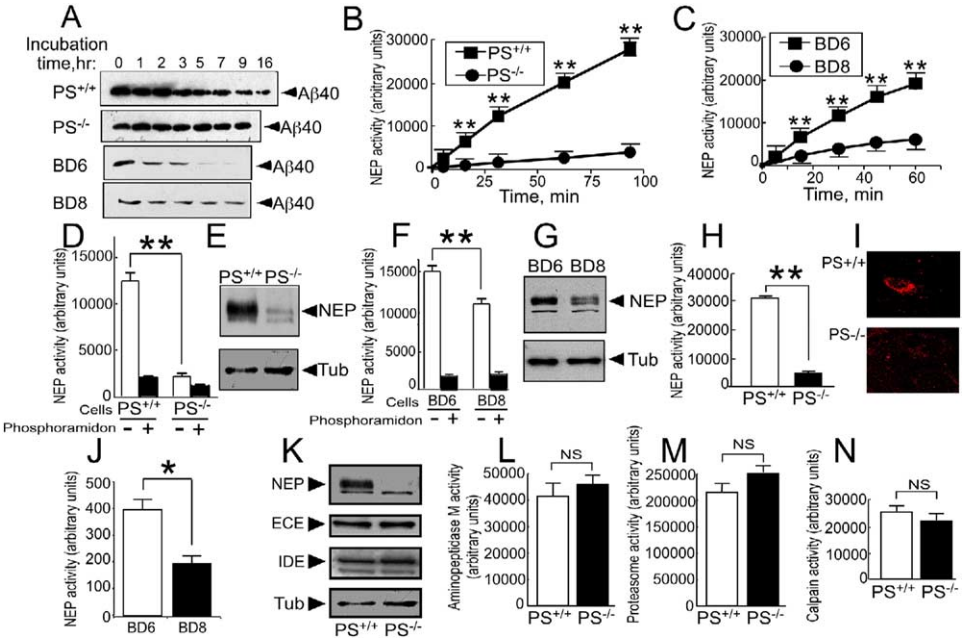

Figure 1. Neprilysin Expression and Activity Are Selectively Lowered in Presenilin-Deficient Cells

(A) Synthetic Aβ40 was incubated for various time periods with the indicated wild-type or PS-deficient cells; then Aβ-related immunoreactivity was analyzed after 16.5% Tris-tricine electrophoresis and Western blot with WO2.

(B–J) Neprilysin activity was measured in fibroblasts (B, D, and H) or blastocyst-derived (C, F, and J) homogenates (B–D and F) or intact cells (H and J). Neprilysin corresponds to total (white bars in [D] and [F]) or phosphoramidon-sensitive (B, C, H, and J) Suc-Ala-Ala-Phe-7AMC-hydrolyzing activity. Neprilysin-like immunoreactivity was monitored in whole homogenates (E and G) or by immunohistochemical labeling on intact fibroblasts (I). Bars represent the mean ± SEM of six (D), nineteen (F), three (H), or sixteen (J) independent determinations. *$p < 0.001$; **$p < 0.0001$.

(K–N) Neprilysin (NEP)-, endothelin-converting enzyme (ECE)-, and insulin-degrading enzyme (IDE)-like immunoreactivities were monitored in homogenates of $PS^{+/+}$ and $PS^{-/-}$ fibroblasts (K). Aminopeptidase M (L), proteasome (M), and calpain (N) activities were measured on the indicated intact cells (L) or in fibroblast cell homogenates (M and N). Bars in (L)–(N) represent the mean ± SEM of ten (L) or three (M and N) independent determinations.

and clearance of Aβ is likely to be delicately regulated, breaking down only in circumstances that lead to the onset of Alzheimer's disease. We show here that although γ-secretase cleavage produces Aβ, the other product of γ-secretase cleavage (AICD) specifically upregulates the transcription of NEP, which in turn, accelerates the degradation of Aβ. This transcriptional signaling pathway therefore provides a simple and elegant physiological mechanism for the regulation of Aβ levels following physiological activation of γ-secretase cleavage of βAPP.

Results

Neprilysin Expression and Activity Are Reduced in Cells Devoid of Presenilins

Aβ40 immunoreactivity decreases in a time-dependent manner upon exposure of exogenous Aβ40 peptide to wild-type fibroblasts and blastocysts ($PS^{+/+}$ and BD6, Figure 1A). This decrease could be blocked by phosphoramidon (Suda et al., 1973), a specific inhibitor of neprilysin (not shown). However, we observed that Aβ40 was not efficiently degraded by PS-deficient fibroblasts or by PS-deficient blastocysts ($PS^{-/-}$ and BD8, Figure 1A). These results raise the possibility that neprilysin activity might be modulated, either directly or indirectly, by the presenilins. This hypothesis was directly supported by the subsequent observation that, in comparison with wild-type cells, PS-deficient cells displayed dramatically lower levels of total neprilysin-like activity, phosphoramidon-sensitive activity, and neprilysin protein expression. In Figures 1D and 1F, comparison of the white bars reveals the difference in total neprilysin-like activity: 12450 ± 934 versus 2148 ± 326 for fibroblasts (Figure 1D; $p < 0.0001$) and 15450 ± 754 versus 11160 ± 672 for blastocysts (Figure 1F; $p < 0.0001$). Similarly, phosphoramidon-sensitive activity is lower in PS-deficient cells: 10480 ± 771 versus 1029 ± 219 for fibroblasts (Figure 1D; $p < 0.0001$) and 13730 ± 749 versus 9149 ± 672 for blastocysts (Figure 1F; $p < 0.0001$). The same held for neprilysin protein expression: 29% ± 5.4% of control expression was observed in $PS^{-/-}$ fibroblasts (Figure 1E, $n = 7$; $p < 0.0001$) and 51% ± 3% of control expression was observed in $PS^{-/-}$ blastocysts (Figure 1G, $n = 11$; $p < 0.0001$). Note that kinetic analyses indicated that NEP activity was significantly lower at all time points in PS-deficient fibroblasts (Figure 1B; $p < 0.0001$) and blastocysts (Figure 1C; $p < 0.0001$).

Because neprilysin is a typical type II membrane-bound peptidase (Roques et al., 1993), we next exam-

ined neprilysin activity on the surface of intact cells, using a cell-impermeable fluorimetric substrate. In this assay, the substrate is cleaved only by enzymes that are present at the cell surface with their catalytic sites facing the extracellular space. In agreement with the studies on whole-cell lysates described above, PS-deficient fibroblasts exhibited a significant 80% reduction of cell membrane neprilysin activity compared to that in wild-type fibroblasts (31130 ± 582 versus 4609 ± 359, Figure 1H; p<0.0001). Furthermore, neprilysin immunoreactivity was poorly detectable at the surface of intact PS-deficient fibroblasts, although it was readily detectable on the surface of wild-type fibroblasts (Figure 1I). A similar reduction in cell membrane neprilysin activity was also observed in PS-deficient blastocysts (BD8), but not in wild-type blastocysts (BD6) (380.7 ± 34 versus 199 ± 25, Figure 1J; p < 0.001).

Presenilin Deficiency Selectively Affects Neprilysin

To assess whether PS deficiency specifically altered neprilysin activity, or whether it also affected other putative Aβ-degrading activities or proteases, we measured the expression of endothelin-converting enzyme and insulin-degrading enzyme (Figure 1K) and the activities of aminopeptidase M, another ectoenzyme (Figure 1L) (Checler, 1993), proteasome (Figure 1M), and calpain (Figure 1N). In sharp contrast to the effects of PS-deficiency on neprilysin, none of these other enzymes were affected by the absence of PS1 and PS2.

Presenilin 1 and Presenilin 2 Affect Neprilysin Transcription

The presenilins directly interact with several unrelated proteins such as nicastrin, Aph-1, and Pen-2, and many of these proteins are destabilized by the absence of the presenilins (for review, see De Strooper, 2003). However, six lines of evidence indicate that the reductions in neprilysin in PS-deficient cells are not due to the loss of a direct, stabilizing interaction between the presenilin and neprilysin proteins, but rather arise from a reduction of neprilysin transcription. First, anti-NEP immunoprecipitates from wild-type fibroblasts do not contain PS1 (Figure 2A) or PS2 (not shown). Second, PS1 and PS2 immunoprecipitation does not deplete supernatants of NEP activity (not shown). Third, residual NEP expression in $PS^{-/-}$ fibroblasts partitioned within cell compartments with the same distribution as in wild-type fibroblasts (Figure 2B), suggesting that PS deficiency did not alter trafficking of NEP in $PS^{-/-}$ fibroblasts. Fourth, neprilysin stability is not affected by PS deficiency (Figure 2C). Fifth, both neprilysin expression and cell surface neprilysin activity can be fully restored by transfection of neprilysin cDNA into PS-deficient fibroblasts (Figure 2D) and into PS-deficient blastocysts (120% ± 4.6% above control mock-transfected cells; p < 0.01; data not shown). Finally, quantitative RT-PCR analyses revealed an approximately 80% reduction in neprilysin mRNA (Figure 3A) (note that overexposure of the gel [lower panel] shows residual mRNA expression).

Taken together, these data suggest that the loss of neprilysin expression in PS-deficient cells arises from impairment in neprilysin transcription. Intriguingly, neprilysin transcription, protein expression, and enzymatic

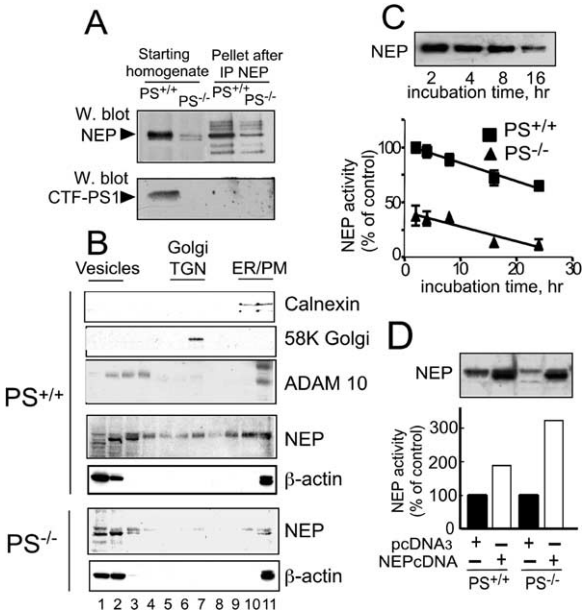

Figure 2. Presenilin Deficiency Does Not Affect Neprilysin at a Post-transcriptional Level

(A) NEP was immunoprecipitated from $PS^{+/+}$ and $PS^{-/-}$ fibroblast homogenates. Immunological complexes were analyzed for their endogenous NEP and PS1-like immunoreactivities. Note that PS1-like immunoreactivity corresponds to the C-terminal maturation product of PS1 (CTF-PS1; Checler, 1999).

(B) Endogenous cell distribution of NEP was analyzed by sucrose density gradient. Note that NEP immunoreactivity is drastically lower in $PS^{-/-}$ fibroblasts (while control β-actin is identical) and that residual NEP behaves as in $PS^{+/+}$, i.e., like the ectoenzyme ADAM10.

(C) $PS^{+/+}$ and $PS^{-/-}$ fibroblasts were treated with cycloheximide to prevent NEP neosynthesis as described in the Experimental Procedures. At the indicated times, NEP activity was fluorimetrically recorded. Note the identical slopes (–1.65 ± 0.22 [$PS^{+/+}$] and –1.35 ± 0.31 [$PS^{-/-}$]), indicating a PS-independent similar decay of NEP (each point is the mean ± SEM of three independent determinations). Upper panel shows NEP immunoreactivity decrease in $PS^{+/+}$ fibroblasts.

(D) Forty-eight hours after transfection in $PS^{+/+}$ and $PS^{-/-}$ fibroblasts, NEP expression (upper panel) and activity (lower panel) were monitored as described in the Experimental Procedures. Bars represent the mean of two independent experiments carried out in duplicate.

activity were not affected in cells devoid of either PS1 only or PS2 only. Thus, normal levels of neprilysin mRNA (Figure 3A), enzymatic activity (Figure 3B), and protein expression (Figure 3C) were observed in $PS1^{-/-}$ fibroblasts (expressing only endogenous PS2) and in $PS2^{-/-}$ fibroblasts (expressing only endogenous PS1). Identical results were achieved when exogenous PS1 or exogenous PS2 were transfected into PS-deficient fibroblasts. Thus, neprilysin mRNA expression, protein expression, and enzymatic activity were equivalently and fully restored in PS-deficient fibroblasts by transient transfection of PS1 and PS2, PS1 only, or PS2 only (Figures 3D and 3E). Control experiments indicate that aminopeptidase M activity was not affected by PS1 or PS2 complementation in PS-deficient fibroblasts (Figure 3F). These data were fully confirmed

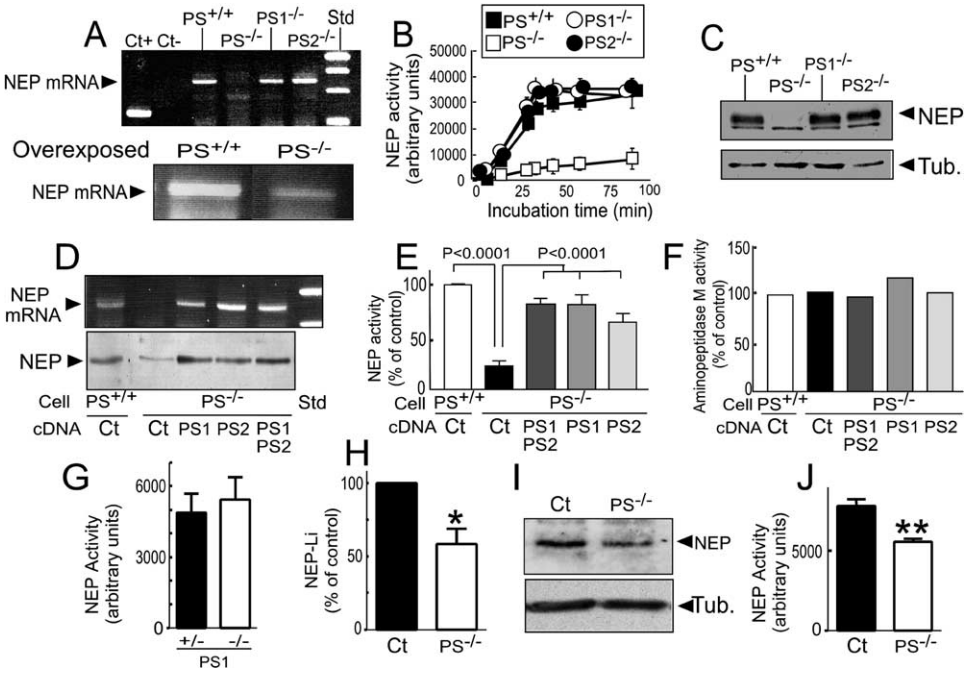

Figure 3. NEP mRNA Expression Is Reduced in PS-Deficient Cells and Restored by Either PS1 or PS2. NEP Is Reduced in Brain Tissue from Conditional Knockout Mice Lacking Both Presenilins

(A) Analysis of NEP mRNA expression by RT-PCR in PS$^{+/+}$, PS1$^{-/-}$, PS2$^{-/-}$, and PS1$^{-/-}$/PS2$^{-/-}$ (PS$^{-/-}$) fibroblasts. Note that only the combined depletion of PS1 and PS2 reduces NEP mRNA expression by 80% (lower panel, an overexposed gel analysis), while PS1 or PS2 invalidation does not affect NEP mRNA expression.

(B and C) PS1$^{-/-}$ and PS2$^{-/-}$ fibroblasts display unaffected NEP activity (B) and expression (C). Data in (B) represent the mean ± SEM of five independent determinations.

(D and E) PS$^{-/-}$ fibroblasts were transiently transfected with PS1, PS2, or both (PS1/2) cDNAs, and then NEP mRNA and protein (D) or activity (E) was monitored. Note that PS1 or PS2 cDNA alone fully restores NEP mRNA expression as well as NEP expression and activity. Bars in (E) represent the mean ± SEM of three independent determinations.

(F) In the same PS$^{-/-}$ transfected cells, aminopeptidase M activity remains unaffected. Bars represent the mean of two independent determinations.

(G–J) PS1$^{-/-}$ (G) and double KO PS1$^{-/-}$PS2$^{-/-}$ (H–J) mice brains were homogenized and examined for NEP activity (G and J) or expression (I). Bars in (H) correspond to the densitometric analysis of NEP expression in three independent determinations; *p < 0.05. Bars in (G) and (J) correspond to the mean of three independent determinations; **p < 0.01.

in vivo because PS1-deficiency did not alter brain neprilysin activity (Figure 3G), while neprilysin expression (Figures 3H and 3I) and activity (Figure 3J) were similarly and significantly reduced in brain tissue from conditional double knockout mice lacking both presenilins (41% ± 9% and 29% ± 2.3% inhibition of NEP expression and activity, respectively, n = 3; p < 0.05 in PS$^{-/-}$ versus control brain). These data therefore lead to the conclusion that PS1 and PS2 may have redundant roles in regulating neprilysin transcription, but depletion of both PS1 and PS2 significantly reduces transcription of this enzyme.

γ-Secretase Inhibitors Reduce Neprilysin Activity in Neuronal and in Wild-Type Cells but Not in PS-Deficient Fibroblasts

The reduction in neprilysin transcription in PS-deficient cells could arise from loss of presenilin-dependent γ-secretase activity or from loss of some other putative activity of the presenilin complexes. To resolve this question, we examined whether neprilysin activity could be directly modulated in wild-type cells by γ-secretase inhibitors. Chronic treatment of wild-type fibroblasts with the γ-secretase inhibitor DAPT (Dovey et al., 2001) led to a 50% inhibition of neprilysin activity (p < 0.0001, Figure 4A). The inhibitory effect was maximal at 48 hr of treatment, a time point at which DAPT was inert on aminopeptidase activity (Figure 4B). Other γ-secretase inhibitors, namely L685,458 (Shearman et al., 2000) or DFK167 (referred to as MW167 in Wolfe et al. [1998]) also elicited significant reduction of neprilysin activity (p < 0.001 and p < 0.05, respectively, Figure 4C), while a control calpain inhibitor (CPI) was totally ineffective (Figure 4C). Importantly, DFK167 also lowers neprilysin activity in TSM1 neurons (30.4% ± 3.8% of inhibition versus control, n = 5; p < 0.0001, Figure 4E) and in primary cultured neurons (56.3% of inhibition, n = 2, Figure 4F). All inhibitors remain inactive on the residual neprilysin activity observed in PS-deficient fibroblasts (Figure 4D) and do not affect in vitro NEP activity (not shown).

AICDs Upregulate Neprilysin Activity and Expression in PS-Deficient Fibroblasts and Blastocysts and Neprilysin Promoter Transactivation

The canonical γ-secretase-mediated hydrolysis liberates the C terminus of Aβ40/42 and concomitantly re-

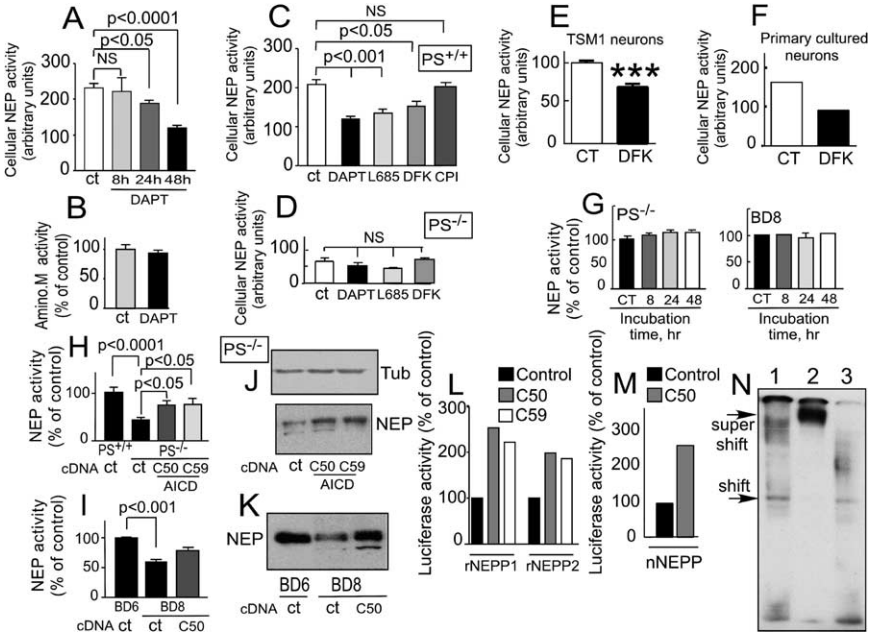

Figure 4. Effect of γ-Secretase Inhibitors and γ-Secretase-Derived βAPP Fragments on NEP Activity and Promoter Transactivation

(A–F) Wild-type ($PS^{+/+}$) fibroblasts were chronically treated by successive additions of DAPT for a total time period of 8, 24, and 48 hr (see Experimental Procedures) (A) or for 48 hr (B) with 2 μM of DAPT, and then NEP (A) or aminopeptidase M (B) activities were fluorimetrically recorded on intact cells. Error bars represent the mean ± SEM of three to six independent determinations. $PS^{+/+}$ (C), $PS^{-/-}$ fibroblasts (D), TSM1 neurons (E), and primary cultured neurons (F) were treated with the indicated inhibitor (DAPT, 48 hr, 2 μM; L685,458, 8 hr, 1 μM; DFK167, 8 hr, 100 μM; calpain inhibitor [CPI], 8 hr, 100 μM), and then the NEP activity of intact cells was measured. Error bars represent the mean ± SEM of three to five independent determinations; ***$p < 0.0001$.

(G–K) PS-deficient ($PS^{-/-}$) fibroblasts or PS-deficient (BD8) blastocyst-derived cells (G) were treated for various time periods with 10 ng/ml of Aβ42, and then NEP activity was fluorimetrically assayed on intact cells. Error bars represent the mean ± SEM of three experiments. $PS^{-/-}$ fibroblasts (H and J) or BD8 cells (I and K) were transiently transfected with empty vector or with the indicated AICD cDNA , and then NEP activity (H and I) or expression (J and K) was monitored. Bars in (H) and (I) represent the mean ± SEM of five independent experiments.

(L and M) The indicated AICD was cotransfected in fibroblasts (L) or in TSM1 neurons (M) with β-gal cDNA and either renal NEP promoters rNEPP1 and rNEPP2 (L) or neuronal NEP promoter nNEPP (M), and then β-galactosidase and luciferase activities were monitored.

(N) HEK293 cells were transfected with AICDC59, Fe65, and Tip60 cDNA , and then nuclear extracts and binding experiments with the 219 bp probe derived from rNEPP were carried out as described in the Experimental Procedures. Lane 1, labeled probe + nuclear extract; lane 2, labeled probe + nuclear extract + Anti-myc; lane 3, labeled probe + nuclear extract + unrelated antibody.

leases the 59 amino acid stub composed of the cytoplasmic C-terminal tail of βAPP referred to as AICDC59 (see Introduction and Figure 8). An additional presenilin-dependent proteolytic cleavage of βAPP and Notch occurs several amino acids downstream (referred to as ε cleavage). This ε cleavage event liberates AICDC50 from APP and a Notch IntraCellular Domain (NICD) from Notch (Gu et al., 2001; Sastre et al., 2001; Weidemann et al., 2002). Because NICD is known to modulate the transcription of several genes, we reasoned that neprilysin transcription might be modulated by one of the γ/ε-secretase-derived products. Exogenous Aβ42 did not modify neprilysin activity in PS-deficient fibroblasts or in PS-deficient blastocysts (Figure 4G). However, transient transfections of AICDC50 or AICDC59 cDNAs increased both neprilysin activity (Figures 4H and 4I) and neprilysin expression (Figures 4J and 4K) in PS-deficient fibroblasts and blastocysts.

In order to link our observation of AICD-induced increase of neprilysin activity and expression to our observation of PS-dependent neprilysin mRNA upregulation, we examined the effect of AICDC50 and AICDC59 on neprilysin promoter transactivation, using various neprilysin promoter elements upstream of a luciferase reporter minigene. Both AICDs dramatically increased the transactivation of two renal neprilysin promoters, rNEPP1 (–385 bp to +147 bp) and rNEPP2 (–263 bp to +145 bp, Figure 4L) in fibroblasts. To confirm AICD-induced transactivation of the neprilysin promoter in a neural cell line, we also cloned the neuronal neprilysin promoter and repeated the luciferase reporter assay. In agreement with the above observations, AICDC50 also transactivated neprilysin promoter in TSM1 neurons (Figure 4M). Supergel shift assay analysis demonstrated that the AICD-potentiated transactivation of the neprilysin promoter indeed appears to be mediated by a direct physical interaction of AICD with the neprilysin promoter (Figure 4N).

AICD-Induced Complementation of Neprilysin Activity Is Potentiated by Fe65 and Tip60 in Fibroblasts and in HEK293 Cells

Several lines of evidence have indicated that the adaptor protein Fe65 modulates the stability of AICD (Kimberly et al., 2001; Kinoshita et al., 2002), thereby potentiating its subsequent nuclear translocation and

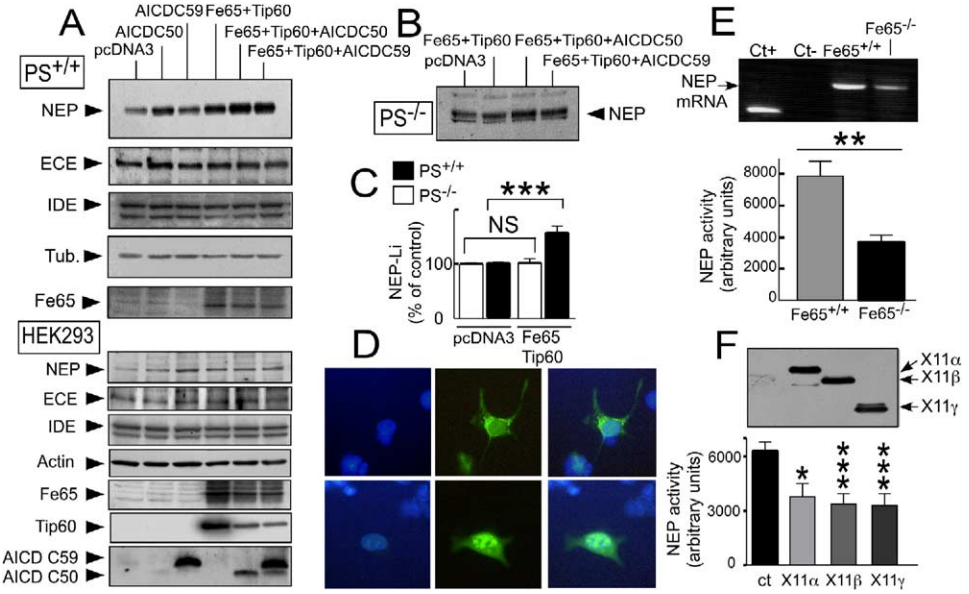

Figure 5. Effect of Fe65 and Tip60 on NEP in Fibroblasts and HEK293 Cells

(A–C) $PS^{+/+}$ ([A], upper panel and [C]) and $PS^{-/-}$ (B and C) fibroblasts were transiently transfected with the indicated mix of cDNAs; then NEP, ECE, IDE, Fe65, and β–tubulin expressions were measured by Western blot. (Note that gel in [B] corresponds to a long exposure in order to visualize any putative effect of Fe65 and Tip60 on residual NEP). Densitometric analyses (C) indicate that transfection of Fe65 and Tip60 cDNAs alone increases NEP expression in $PS^{+/+}$ ($p < 0.0005$ when compared to vector alone) but not in $PS^{-/-}$. Error bars in (C) represent the mean ± SEM of four independent determinations. (A, D, and F) HEK293 ([A], lower panel, [D], and [F]) were transiently transfected with the indicated mix of cDNAs (A) or indicated X11 cDNA (F); then NEP, ECE, IDE, Fe65, actin, AICDC50, AICDC59, and X11 expressions were measured by Western blot. In (D), AICDC59-like immunoreactivity was assessed by immunohistochemistry after transfection of AICDC59 alone (upper panels) or together with Fe65 and Tip60 (lower panels) in HEK293 cells. Note the increase of AICDC59 expression and the nuclear redistribution of AICDC59-like immunoreactivity (shown by merge with nuclear DAPI label [left panels]) triggered by Fe65 and Tip60 cDNA transfections. (E) NEP mRNA (upper panel) and activity (lower panel) are decreased by Fe65 deficiency in fibroblasts. Bars in (E) and (F) represent the mean ± SEM of four (E) or five (F) independent experiments. *$p < 0.05$; **$p < 0.01$; ***$p < 0.001$.

interaction with the histone acetyltransferase Tip60 (Cao and Südhof, 2001). We therefore examined whether Fe65 and Tip60 could (1) influence neprilysin by modulating endogenous AICD in wild-type fibroblasts and in HEK293 cells and (2) potentiate AICD-induced increase in neprilysin activity.

Fe65 and Tip60 transfection enhanced neprilysin expression and activity in $PS^{+/+}$ fibroblasts (Figure 5A [upper panel] and Figure 5C; $p < 0.0005$) and in HEK293 cells (Figure 5A [lower panel]), but not in PS-deficient cells (Figures 5B and 5C), indicating that Fe65 and Tip60 augment neprilysin expression through functional interaction with an endogenous PS-dependent product. In wild-type $PS^{+/+}$ fibroblasts, the cotransfection of Fe65 and Tip60 with either AICDC50 or AICDC59 cDNA increased neprilysin expression when compared to AICDs cDNA transfection alone (Figure 5A). This was accompanied by an augmentation of AICDC50 and AICDC59 immunoreactivities (Figure 5A [lower panel]) and by a clear translocation of AICDC59 (Figure 5D) and AICDC50 (not shown) into the nuclei of HEK293 cells and $PS^{+/+}$ fibroblasts (not shown). Similar potentiation of neprilysin expression by Fe65 and Tip60 transfection was also observed in AICD-transfected PS-deficient fibroblasts (136% ± 6%, AICDC50+Fe65+Tip60 versus AICDC50 alone and 135% ± 6.2%, AICDC59+Fe65+Tip60 versus AICDC59 alone; $p < 0.0005$). Interestingly, AICDC50 and AICDC59 increase renal neprilysin promoter transactivation in HEK293 cells (not shown), a phenotype further potentiated by Fe65 and Tip60 (142.9% ± 19% and 174.9% ± 19% for AICDC50+Fe65+Tip60 and AICDC59+Fe65+Tip60 versus control, respectively, $n = 3$; $p < 0.05$). Fe65 and Tip60 (either alone or in combination with AICDs) had no effect on the expressions of endothelin-converting enzyme and insulin-degrading enzyme in $PS^{+/+}$ fibroblasts and HEK293 cells (Figure 5A), a result that is in agreement with the experiments described above showing that the presenilin-dependent enhancement of Aβ degradation is specific to neprilysin (see Figure 1). In order to examine whether Fe65 could be a limiting factor for expression of neprilysin, we examined the activity of neprilysin in p97Fe65-deficient mice fibroblasts (Wang et al., 2004). Abolition of p97Fe65 diminished neprilysin activity (52% ± 5.9% of decrease in $Fe65^{-/-}$ versus control fibroblasts, $n = 4$; $p < 0.01$) (Figure 5E) and mRNA expression (27% ± 1.5% of decrease in $Fe65^{-/-}$ versus control fibroblasts, $n = 3$; $p < 0.005$) (Figure 5E).

Interestingly, the overexpression of X11α, X11β, and X11γ that triggers opposite effects on Aβ recovery when compared to Fe65 (Borg et al., 1998; Sastre et al., 1998; Lee et al., 2003) decreased neprilysin activity in HEK293 cells (40%, 46%, and 47% of inhibition of neprilysin activity compared to control for X11α, X11β, and X11γ, respectively, $n = 5$) (Figure 5F).

βAPP and APLPs Complement Each Other to Control Neprilysin In Vitro and In Vivo

To test whether the endogenous PS-dependent product controlling neprilysin activity was indeed AICD, we

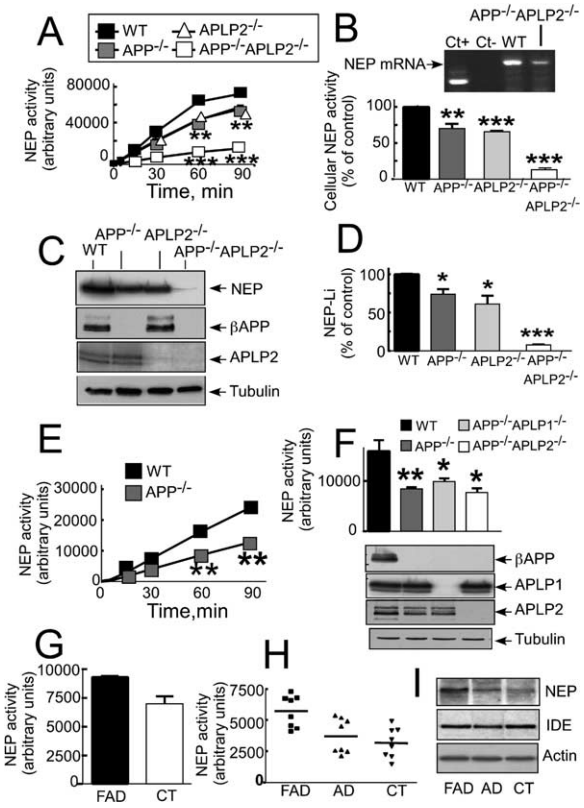

Figure 6. NEP Expression and Activity Are Affected by APP, APLP1, and APLP2 Deficiencies In Vitro and In Vivo and by FAD Mutations in Brain Tissues

NEP activity in homogenates (A and E–H) or intact cells (B) and expression (C, D, and I) were monitored as described in the Experimental Procedures in the indicated single or multiple KO fibroblasts (A–D) or in mice (E and F) or Alzheimer's (G–I) brain tissues. (G) NEP activity in L392V-PS1 and control brain. Activity (H) and expression of NEP and IDE (I) in L235P-PS1 and F386S-PS1 cases (FAD), two sporadic cases (AD), and control brains (CT). Bars in (B), (F), and (G) represent the mean ± SEM of three to seven independent determinations. Insert in (B) corresponds to RT-PCR NEP mRNA analysis in wild-type (WT) and APP$^{-/-}$APLP2$^{-/-}$ fibroblasts. Bars in (D) correspond to the densitometric analysis of NEP expression and represent the mean ± SEM of three determinations. *p < 0.05; **p < 0.005; ***p < 0.0001.

examined neprilysin activity and expression in βAPP-deficient fibroblasts. βAPP$^{-/-}$ fibroblasts exhibit a similarly significant reduction of neprilysin activity (30% ± 7.6% [n = 7; p < 0.005; Figure 6A] and 31% ± 6.7% [n = 3; p < 0.001; Figure 6B] reduction in homogenates and intact cells, respectively, versus control activity) that fully matched the reduction in NEP expression (26.1% ± 6.9% reduction, n = 3; p < 0.05; Figures 6C and 6D). Neprilysin activity is fully restored by βAPP cDNA transfection in APP$^{-/-}$ fibroblasts (125.6 ± 6 of control, n = 4; p < 0.01; Figure 7A). It is of interest that loss of βAPP expression in APP$^{-/-}$ mouse brain triggers a significant reduction in neprilysin activity (47% ± 3.5% in APP$^{-/-}$ versus control, n = 4; p < 0.005; Figures 6E and 6F). This suggests that derivatives of βAPP might also control cerebral neprilysin in vivo and supports the notion that a presenilin-dependent, γ-secretase-mediated cleavage product of APP, namely AICD, is a physiological regulator of neprilysin transcription both in vitro and in vivo. However, it should be noted that the extent of inhibition of neprilysin activity appeared lower in βAPP$^{-/-}$ cells than in PS$^{-/-}$ fibroblasts. Therefore, we examined whether neprilysin activity and expression could be controlled by other βAPP-like proteins. Interestingly, APLP2-deficiency in fibroblasts triggers a decrease in both neprilysin activity and expression that is similar to the reductions observed in βAPP$^{-/-}$ cells (Figures 6A–6D). Neprilysin activity is fully restored by APLP2 cDNA transfection in APLP2$^{-/-}$ fibroblasts (125.1 ± 6.9 of control, n = 3; p < 0.05; Figure 7A). However, the absence of both βAPP and APLP2 in fibroblasts resulted in an even more dramatic reduction in neprilysin activity and expression (80% ± 2.6% reduction of activity in homogenate, n = 8; p < 0.0001; Figure 6A; 87% ± 2.% reduction of activity on intact cells, n = 6; p < 0.0001; Figure 6B; and 92% ± 0.7% reduction of expression in APP$^{-/-}$APLP2$^{-/-}$ versus control fibroblasts, n = 3; p < 0.0001; Figures 6C and 6D), while ECE-like and IDE-like immunoreactivities remained unaffected (not shown). Importantly, double βAPP/APLP2 deficiency also led to decreased NEP mRNA expression (30% reduction in two independent experiments, Figure 6B [inset]). Of most interest is our observation that cotransfection of Tip60 and Fe65 cDNAs drastically increase neprilysin activity in wild-type fibroblasts, but not in APP$^{-/-}$APLP2$^{-/-}$ doubly deficient fibroblasts (Figure 7B). However, AICDC50 still potentiates transactivation of rNEPP1 and rNEPP2 promoters in APP$^{-/-}$ APLP2$^{-/-}$ fibroblasts (Figure 7C).

This apparently synergistic effect led us to hypothesize that APP and APLP2, which have homologous C termini, could partially complement each other for the control of neprilysin expression. However, it should be noted that the extent of inhibition of neprilysin activity in brain (52% ± 9.8% in APP$^{-/-}$APLP2$^{-/-}$ versus control, n = 4; p < 0.05; Figure 6F) was lower than that observed in the corresponding APP$^{-/-}$APLP2$^{-/-}$ double knockout fibroblasts. This could be due to another protein that would complement APP and APLP2 function in brain but not in fibroblasts. In this context, it is noteworthy that, unlike in the brain, fibroblasts totally lack the βAPP family member APLP1 (not shown). Therefore we examined whether the γ-secretase-derived fragments of APLP1 (ALID1) and APLP2 (ALID2) could complement neprilysin activity in APP$^{-/-}$APLP2$^{-/-}$ fibroblasts. Indeed, both ALID1 and ALID2 significantly increase neprilysin activity in APP$^{-/-}$APLP2$^{-/-}$ fibroblasts (142.1 ± 8, n = 3; p < 0.005 for ALID1 and 138.8, n = 3; p < 0.005 for ALID2, versus control; Figure 7D). The fact that APP$^{-/-}$, APP$^{-/-}$APLP1$^{-/-}$, and APP$^{-/-}$APLP2$^{-/-}$ brains all display similar reductions in neprilysin activity (Figure 6F) indicate that all the members of the APP family control cerebral neprilysin transcription in vivo. It should be noted, however, that the mice brains devoid of APP, APLP1, and APLP2 do not exhibit enhanced neprilysin decrease when compared to double KO brains (not shown). This suggests that, besides AICD/ALID-regulated neprilysin expression, there exists also a constitutive APP/APLP-independent cerebral NEP activity.

In order to establish whether the control of neprilysin activity was restricted to the APP-related ICDs, we next examined the putative effect of other PS-dependent γ-secretase-mediated products. Thus, NICD is the in-

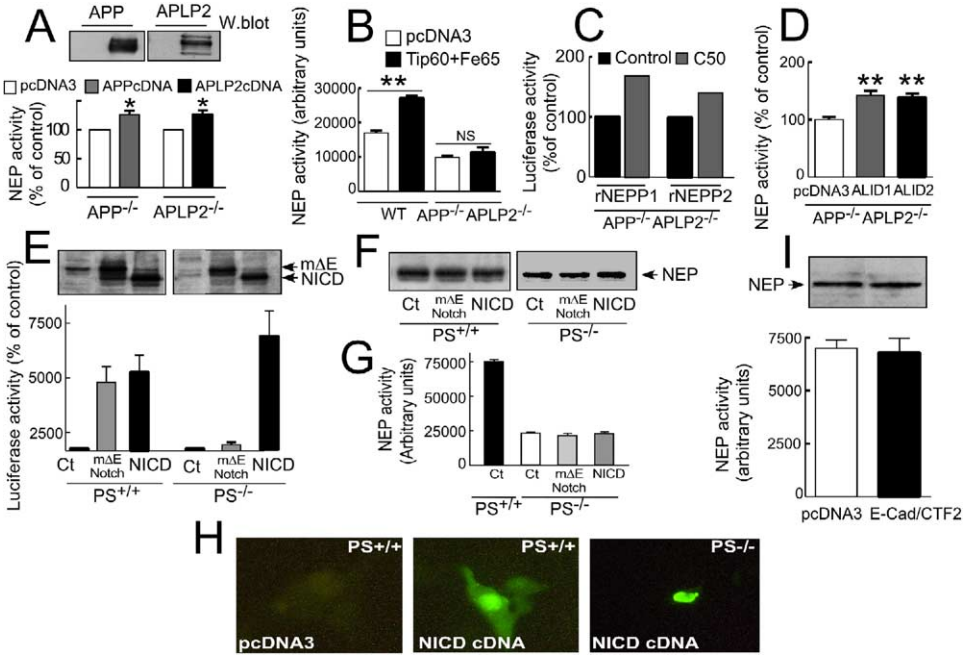

Figure 7. Neprilysin Activity Is Modulated by ALID1 and ALID2 but Not by NICD or E-Cad/CTF2

APP$^{-/-}$ (A), APLP2$^{-/-}$ (A), or APP$^{-/-}$APLP2$^{-/-}$ (B–D) fibroblasts were transfected with empty pcDNA3 vector or indicated cDNAs; then NEP activity (A, B, and D) or transactivation of rNEPP1 and rNEPP2 promoters (C) were monitored as described in the Experimental Procedures. Error bars in (A), (B), and (D) represent the mean ± SEM of three to four independent experiments. *p < 0.05; **p < 0.005. (E–G) The indicated fibroblasts were transiently cotransfected with 4XCBF-luciferase and β-gal cDNAs in combination with either empty vector (Ct) or cDNAs encoding myc-tagged mΔENotch or myc-tagged NICD, and then mΔENotch and NICD (E) or NEP (F) expressions were assayed by Western blot in the indicated cell lines, and luciferase (E) or NEP (G) activities were measured as described in the Experimental Procedures. Bars in (E) and (G) represent the mean ± SEM of three to four independent experiments. NICD expression was also estimated by immunohistochemistry in PS$^{+/+}$ and PS-deficient fibroblasts (H). Note a clear dense label of NICD in the nucleus. (I) E-Cad/CTF2 does not modulate NEP expression and activity in HEK293 cells. Bars in (I) represent the mean ± SEM of seven independent experiments.

tracellular fragment liberated from Notch upon γ-secretase cleavage. To test whether NICD might also affect neprilysin activity, we created fibroblast- and blastocyst-derived cell lines transiently expressing the 4XCBF-luciferase reporter gene. In agreement with previously published works (Herreman et al., 2000; Zhang et al., 2000), the transient cotransfection of mΔENotch (which generates NICD upon γ-secretase cleavage) led to a robust transcriptional activation in wild-type fibroblasts (Figure 7E) and blastocyst-derived cells (not shown), but not in the equivalent PS-deficient cells (Figure 7E). However, transfection of NICD itself into wild-type and PS-deficient cells induced NICD protein expression (Figure 7E), favored nuclear localization of NICD (Figure 7H), and increased luciferase activity (Figure 7E). These control experiments therefore established that NICD was indeed functionally expressed in our experimental system. However, regardless of the cell system used, mΔENotch and NICD were unable to restore neprilysin expression (Figure 7F) or neprilysin activity (Figure 7G) in PS-deficient cells. Furthermore, the γ-secretase-derived C-terminal products of E-Cadherin (E-Cad/CTF2, Figure 7I) (Marambaud et al., 2002) and N-Cadherin (N-Cad/CTF2, not shown) (Marambaud et al., 2003) were also unable to affect neprilysin expression and activity. Thus, unlike AICDs and ALIDs, NICD and E- and N-Cad/CTF2 did not complement neprilysin activity in PS$^{-/-}$ cells. Taken together, these data indicate that the complementation of neprilysin function by γ-secretase-derived products is specifically elicited by ICDs of the βAPP family members.

Neprilysin Expression and Activity Are Increased in Alzheimer's Brains of Genetic Origin

We have examined the neprilysin activity of control human brains and compared them to brain samples of sporadic or genetic AD origin. Neprilysin activity (Figures 6G and 6H) and expression (Figure 6I) were not statistically different between control (CT) and sporadic AD brains, while Familial Alzheimer's disease (FAD) brains harboring PS1 mutations displayed higher activity (Figures 6G and 6H) and expression (Figure 6I). Interestingly, insulin-degrading enzyme (IDE) was not altered in FAD brains (Figure 6I).

Discussion

Several lines of evidence strongly suggest that neprilysin (Hauss-Wegrzyniak and Wenk, 2002; Hama et al., 2001; Marr et al., 2003; Leissring et al., 2003; Iwata et al., 2001), endothelin-converting enzyme (ECE; Eckman et al., 2003), and insulin-degrading enzyme (IDE; Farris et al., 2003) could participate in the catabolism of Aβ peptides. We show here that neprilysin transcription,

expression, and enzymatic activity are dramatically reduced in non-neuronal and neuronal cells when they are devoid of PS1 and PS2 and that this phenotype can be mimicked by γ-secretase inhibitors. We have shown that the presenilins control NEP activity at a transcriptional level and that PS deficiency does not affect the expression of IDE, ECE, or other widely distributed intracellular (calpain and proteasome) or ectopeptidase (aminopeptidase M) activities. We have also shown that neprilysin expression and activity are significantly reduced in brain tissue from mice lacking PS1 and PS2 (Saura et al., 2004), indicating that the presenilins also control cerebral neprilysin transcription, expression, and activity in vivo. This highly specific and physiological relationship between the presenilins and neprilysin strongly argues for a major evolutionary and functional role of neprilysin in the physiological catabolism of Aβ, but does not preclude a role for other enzymes in Aβ catabolism.

The molecular mechanisms by which the presenilins regulate neprilysin transcription would appear, from the data presented here, to involve the C-terminal intracellular domains of APP and APLP proteins (AICDs and ALIDs). Thus, we have clearly established that deficiency of βAPP, APLP1, or APLP2 drastically reduces neprilysin expression and activity in both fibroblasts and in brain tissues. We have specifically shown that Aβ42 and the γ-secretase-derived products of Notch, E-cadherins, and N-cadherins do not support this activity. Furthermore, the Fe65 adaptor protein (which binds to the GYENPTY motif in the cytoplasmic tail of βAPP/AICD [King and Turner, 2004]) and Tip60 clearly potentiate the AICD-induced upregulation of neprilysin in wild-type fibroblasts but not in PS$^{-/-}$ and APP$^{-/-}$/APLP2$^{-/-}$ cells.

It has been previously reported that Fe65 and Tip60 stabilize AICD and favor its translocation to the nucleus (Kimberly et al., 2001; Kinoshita et al., 2002). Our experiments have shown that AICD translocates to the nucleus in the presence of Fe65 and Tip60 and transactivates neuronal and renal neprilysin promoters in TSM1 neurons, HEK293 cells, and APP$^{-/-}$/APLP2$^{-/-}$ fibroblasts, respectively. Furthermore, Supergel shift analysis indicates that AICDC59 interacts physically with the neprilysin promoter in the presence of Fe65 and Tip60. Interestingly, X11, which clearly reduces γ-secretase cleavage of βAPP, also drastically reduces neprilysin activity. Therefore, Fe65 and X11, which trigger opposite effects on Aβ production, also elicit an opposite phenotype in neprilysin regulation.

Altogether, the similar decrease in neprilysin activity and expression triggered by the absence of PS or APP/APLPs, the analogous absence of control of neprilysin by Fe65 and Tip60 in these invalidated fibroblasts, and the opposite phenotype observed with Fe65 and X11 all lead to the firm suggestion that the endogenous γ-secretase-dependent fragments controlling neprilysin are indeed AICD/ALIDs.

The redundant role of PS1 and PS2 in regulating neprilysin transcription contrasts with their overlapping but not redundant roles in modulating Aβ peptide and Notch signaling. Thus, PS2 deficiency alone does not affect γ-secretase-mediated production of Aβ or Notch in vivo (Herreman et al., 1999). However, PS1 deficiency drastically reduces both Aβ production and Notch signaling (De Strooper et al., 1998). We hypothesize that in PS1$^{-/-}$ fibroblasts and brain tissue, APLP1 and APLP2 could undergo γ-secretase-like cleavage by residual endogenous PS2, thus complementing AICD function, and thereby control neprilysin expression and activity. Because APLPs lack the Aβ sequence (although Aβ-like peptides seem to be generated from APLP2), their PS2-dependent cleavage would not compensate for Aβ reduction that is triggered by PS1 deficiency. In this context, the resulting phenotype would be a reduction in Aβ production but with unaltered or weakly modified neprilysin levels. Alternatively, we hypothesize that there is likely to be both a constitutive (AICD-independent) basal expression of NEP and an inducible (AICD-dependent) expression of NEP, as suggested by residual NEP activity in triple KO (APP$^{-/-}$APLP1$^{-/-}$APLP2$^{-/-}$) mice brains (see Results). In PS1$^{-/-}$ fibroblasts and in PS1$^{-/-}$ brain tissue, this constitutive level of expression, together with the cumulative effects of residual AICD and ALIDs generated from APP, APLP1, and APLP2 by the PS2 γ-secretase activity, could be sufficient to maintain neprilysin expression and activity in PS1$^{-/-}$ cells. In contrast, for Notch, there is both absence of constitutive basal expression of Notch-targeted genes and a lack of redundancy in alternate signaling molecules. Another possibility could be that NEP transcription is preserved in PS1$^{-/-}$ cells because APLPs γ-secretase cleavage is not affected to the same extent as APP by PS1 deficiency. However, to our knowledge, there is currently no data to support the notion that PS1 and PS2 have differential/preferential effects on γ-secretase cleavage of APP, APLP1, and APLP2.

The experiments described here do more than simply confirm the previously and widely held suspicion that AICD, like NICD, might act as a signaling molecule involved in transcriptional activation. The experiments here depict an elegant and unusual mechanism by which Aβ levels are controlled. Thus, βAPP is proteolytically processed by presenilin-dependent γ-secretase, which generates two distinct types of catabolites, Aβ and AICD (Figure 8). One of these products, AICD, then controls the lifetime of the other product, Aβ, by selectively activating the transcription of an enzyme (neprilysin) capable of degrading that other product. Thus, γ-secretase activity directly controls Aβ production and then indirectly modulates its degradation. To our knowledge, a similar "self-contained" mechanism for regulating the degradation of enzyme products has not been described previously; (NB: this does not preclude AICDs from also activating other genes).

If Aβ production and degradation are tightly linked, this raises the question of why Aβ accumulates in AD. The net accumulation of Aβ in AD pathology likely reflects the cumulative effect of multiple events acting on production, fibrillogenesis, and degradation. In many forms of AD, especially the late-onset sporadic forms, it has not been shown that there is increased β- and γ-secretase activity. In fact, some have suggested that these forms may reflect defective degradation of Aβ (Iwata et al., 2001; Leissring et al., 2003). Therefore, AICD levels are likely to be unchanged in these late-onset forms of AD, and as a result, the AICD-mediated ability to upregulate neprilysin activity would not be ef-

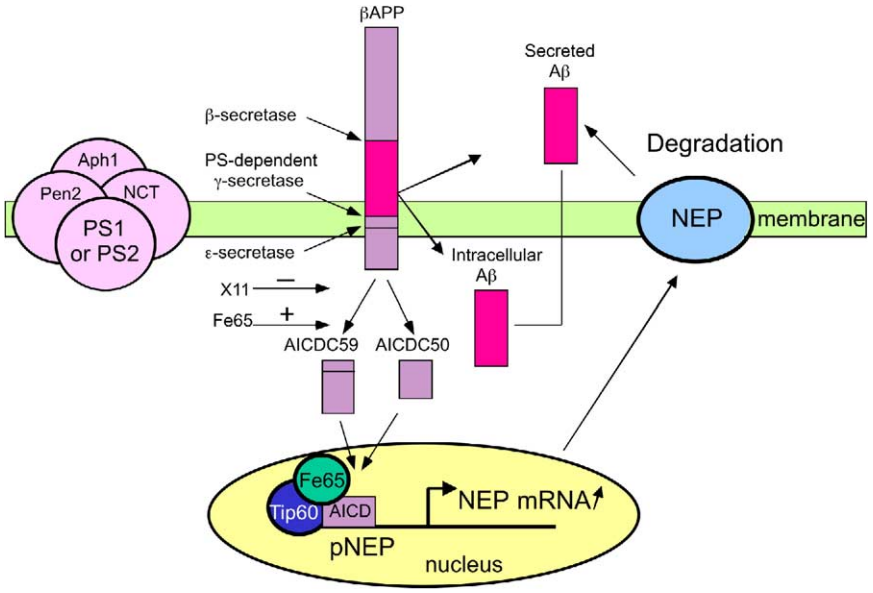

Figure 8. Model for PS-Dependent Transcriptional Activation of NEP by the βAPP-Intracellular Domain

βAPP undergoes proteolysis by various secretases. Aβ peptide is released by the sequential cleavages triggered by β- and γ-secretases in the intracellular compartment from which it can be secreted. Once secreted, Aβ is degraded by the ectopeptidase named neprilysin (NEP), a type II integral protein with catalytic domain facing the extracellular space. Presenilin-dependent γ-secretase cleavage is triggered by a multiproteic complex composed of presenilin 1 (PS1) or presenilin 2 (PS2), nicastrin (NCT), Aph1, and Pen2. γ-secretase contributes to an additional cleavage, referred to as ε cleavage, that takes place slightly downstream from the γ-secretase site. The action at γ and ε sites gives rise to AICDC59 and AICDC50, respectively. AICDs interact with Fe65 and Tip60 to form an active complex activating NEP mRNA transcription. Increased NEP activity, in turn, leads to increased Aβ degradation.

ficiently brought into play to protect the brain. In contrast, in those cases of AD arising from mutations in APP and PS1, which activate γ-secretase and AICD production, the principal effect is to produce longer Aβ isoforms such as Aβ42. However, although Aβ40 is efficiently degraded by NEP, Aβ42 is degraded by NEP both in vitro and in vivo at a 6-fold lower rate, (Shirotani et al., 2001). As a result, the upregulation of AICD (and thus, NEP expression), which would be anticipated in subjects with presenilin mutations, would not completely abolish the accumulation of Aβ42 in these cases. It should be noted that, in agreement with the above hypothesis, neprilysin expression and activity were higher only in brain tissues with familial Alzheimer's disease linked to various presenilin-1 mutations, while sporadic AD cases displayed neprilysin levels similar to those exhibited by normal brain tissues (Figures 6G–6I). Interestingly, PS1 mutations selectively affect neprilysin and do not alter insulin-degrading enzyme expression.

The above observations are also of direct practical interest because they indicate the possibility of new avenues for controlling Aβ levels without directly affecting γ-secretase. This latter concept is important because of the various developmental and postnatal side-effects associated with the inhibition of γ-secretase-mediated cleavage of other signaling molecules, including Notch (Sisodia and St. George-Hyslop, 2002; Haass and De Strooper, 1999). Our work now suggests that Aβ levels might be modulated by directly increasing neprilysin expression, using AICD or small molecule mimics of AICD. Upregulation of neprilysin by transgenic overexpression, at least to modest levels, appears to be sufficient to reduce brain Aβ levels and to pose few toxic side effects (Leissring et al., 2003). This strategy would also circumvent the other side effects of γ-secretase inhibitors, including the potentially self-defeating effect of reducing AICD and thus preventing NEP-mediated degradation of Aβ.

Experimental Procedures

Cell Culture and Transfections

Primary cultured neurons, HEK293 cells, telencephalon murine (TSM1) cell lines, blastocyst-derived cells, PS-, βAPP-, and p97Fe65-deficient fibroblasts were obtained and cultured as previously described (Vincent et al., 1996; De Strooper et al., 1999; Zhang et al., 2000; Herreman et al., 2000 Armogida et al., 2001; Leissring et al., 2002; Wang et al., 2004). Mouse embryonic fibroblasts derived from APLP2 or APP/APLP-deficient mouse embryos and their littermates (Heber et al., 2000) were immortalized with the large T antigen of SV40. Several clonal lines were established and cultured in DMEM/10% fetal calf serum containing 2 mM glutamine and 50 μM β-mercaptoethanol. Transient transfections were carried out with DAC 30 (Eurogentec).

Fluorimetric Assays of Enzymatic Activities

NEP activity was measured on intact cells or in cell homogenates with Suc-Ala-Ala-Phe-7AMC in the absence or presence of phosphoramidon as described previously (Checler, 1993). When NEP activity was measured in brain tissues, brains were homogenized in Tris 10 mM (pH, 7.5) and centrifuged; then pellets were resuspended in initial volumes of homogenization buffer, and activity was measured as above. Aminopeptidases B and M, calpain, and

proteasome activities were measured as previously described (Checler, 1993).

Effect of Aβ42 and γ-Secretase Inhibitors on NEP Activity on Intact Cells

Chronic treatment of wild-type $PS^{+/+}$ fibroblasts with DAPT was achieved by addition of 2 μM of the inhibitor at 0, 4, 8, 16, 20, 24, 40, 44, and 48 hr, and NEP activity was measured on intact cells at 8, 24, or 48 hr as described above. The effect of L685,458 (1 μM), DFK167 (100 μM), or Aβ42 (10 ng/ml) on NEP activity was also assessed, as indicated above, in intact wild-type fibroblasts, TSM1 neurons, and primary cultured neurons.

Coimmunoprecipitation Experiments of Endogenous NEP and PS1

Cells were harvested in lysis buffer (50 mM Tris-HCl [pH, 7.5], 150 mM NaCl, 5 mM EDTA, 0.5% Triton X-100, and 0.5% Deoxycholate), and then 500 μg of protein was diluted in 1:2 RIPA 2X buffer and incubated overnight at 4°C with a 2000-fold dilution of anti-neprilysin 18B5 antibody together with protein A-sepharose. After centrifugation, pellets were resuspended in loading buffer containing SDS, submitted to 8% (NEP) or 12% (PS1) SDS-polyacrylamide gel electrophoresis, and Western blot analysis. Membranes were probed with 18B5 or anti-PS1 antibody. Immunoreactive bands were identified with anti-rabbit peroxidase (Immunotech) or anti-mouse peroxidase (Amersham Life Science) antibodies, followed by electrochemiluminescence (ECL) as previously described (Alves da Costa et al., 2002) (Amersham Pharmacia Biotech).

Subcellular Fractionation by Sucrose Gradient

Four 100 mm diameter dishes of confluent $PS^{+/+}$ and $PS^{-/-}$ fibroblasts were homogenized with a dunce homogenizer in 0.25 M sucrose and 10 mM Tris-HCl (pH, 7.4) containing 1 mM $MgAc_2$ and a protease inhibitor mixture (Sigma). Equal amounts of proteins (3.8 mg) of each homogenate were loaded on top of a step gradient. After centrifugation, eleven 1 ml fractions were collected from the top of each gradient. Proteins contained in 100 μl of each fraction were precipitated with 5 volumes of methanol overnight at 4°C, resuspended in sample buffer, and heated for 5 min at 95°C. Neprilysin was assayed by Western blot as described below. The full characterization of cell markers has been described elsewhere (Luo et al., 2003).

SDS/PAGE and Western Blot Analyses

NEP, β-tubulin, β actin, ECE, IDE, mΔENotch, NICD, βAPP, APLP1/2, X11α, β, and γ, Fe65, and Tip60 were separated on 8% Tris-glycine gels, while Aβ40, AICDC50, and AICDC59 were analyzed on 16.5% Tris-tricine gels. Proteins were transferred onto Hybond-C membranes and then probed with the following antibody: 18B5 (anti-neprilysin; Dr. G. Boileau), anti-mouse ECE 32 and anti-human ECE 27 (Dr. K. Isobe), polyclonal anti-mouse IDE and anti-APLP1 and APLP2 (EMD Biosciences), anti-human IDE (Dr. F. Authier), 9E10 anti-myc antibody (myc-tagged mΔENotch, NICD, AICDC50, and AICDC59), monoclonal 22C11 (βAPP), polyclonal anti-Fe65 (Dr. L. Mercken), anti-HA (Tip60-HA), and WO2 antibody (Aβ40). Immunological complexes were revealed with anti-rabbit peroxidase or anti-mouse peroxidase antibodies, followed by electrochemiluminescence (Alves da Costa et al., 2002).

RT-PCR Analysis of NEP mRNA

Total RNA was extracted and purified with the SV Total RNA Isolation System (Promega). For each RT-PCR reaction, 500 ng of RNA was used. To amplify mouse neprilysin cDNA, the forward primer was 5′-AGCCTCTCTGTGCTTGTCTTGC-3′ and the backward primer was 5′-CACTCATAGTAGCCT-CTGGAAGGG-3′, yielding a 614-bp product. RT-PCR reactions were performed with the Access RT-PCR System (Promega). The reverse transcription was done at 48°C for 45 min, followed by a denaturation step at 94°C for 2 min. PCR reactions were performed at 94°C for 30 s, 55°C for 1 min, and 68°C for 2 min during 40 cycles, followed by a final extension of 7 min at 68°C. RT-PCR products were analyzed on a 1% agarose gel stained with ethidium bromide.

Cloning of AICDC50 and AICDC59

pcDNA4-AICDC59 was constructed by PCR amplification of the indicated coding sequence of βAPP from pcDNA4-βAPP (Chen et al., 2002) using the primers: 5′-TTTGGTGGAATTCATGATAGCGACA GTGATC GTCATCACC-3′ and 5′-TTTACCTCG-AGCGTTCTGCAT CTGCTCAAAG AAC-3′. The initial methionine was artificially introduced (underlined). The product was digested with EcoRI/XhoI and subcloned into the EcoRI/XhoI site of pcDNA4 (Invitrogen) containing the coding sequence for the Myc epitope at C terminus. The construct was confirmed by sequencing. pcDNA4-AICDC50 was constructed using the primers 5′-TTTGGTGGAATTCATGGTGATG CTGAAGAAGAAA-CAGTAC-3′ and 5′-TTTACCTCGAGCGTT CTG CATCTGCTCAAAGAAC-3′. The amplified product was ligated into the pcDNA4 vector as described above.

Neuronal NEP Promoter Cloning and NEP-Luciferase Reporter Constructs

The longest 5′-UTR for neprilysin is 98 bp, suggesting that the transcription start site is at least 4452 bp from the ATG site. To clone the promoter regulatory elements, a 2500 bp DNA fragment upstream of the presumed transcription start site was amplified from human genomic DNA using the forward primer 5′-GCACTATAGC ATTTTTAAAGG-3′ and the reverse primer 5′-TGCTCCAGCCTGCT CTCGGTC-3′ (NCBI accession number AC117384, positions 71,677–74,176, which corresponds to −6951 to −4452 from the ATG site). The fragment was inserted into the pCR2.1 vector (Invitrogen) and subcloned between BamHI and XbaI restriction sites into pBluescript vector (Stratagene) to introduce an additional XhoI site. NEP promoter containing insert was then excised by XhoI digestion and religated into pGL-2 vector (Promega). The subcloned fragment was sequenced and its direction and the absence of mutational sequences were confirmed. Two renal NEP promoter constructs rNEPP1 (−385 bp to +147 bp) and rNEPP2 (−263 bp to +145 bp) in frame with luciferase have been previously reported (Ishimaru et al., 1997).

Measurements of NEP Promoter Transactivation

Neuronal and renal neprilysin promoter-luciferase constructs were cotransfected with βgal reporter cDNA in fibroblasts, TSM1 neurons, and HEK293 cells in the absence or presence of AICDs cDNA. Forty-eight hours after transfection, luciferase and βgal activities were measured according to previously described procedures (Paitel et al., 2004).

Immunofluorescence Analysis

Cells (grown on glass coverslips) were transfected with AICDs or NICD cDNAs. Forty eight hours after transfection, cells were fixed for 20 min with 1.5% paraformaldehyde and permeabilized for 5 min with 0.1% Triton X-100. After three washes, cells were incubated with the primary antibody for 4 hr at room temperature. Cells were then washed three times with PBS and incubated for 1 hr at room temperature with the Alexa488-labeled goat anti-mouse antibody (Interchim). Coverslips were washed and mounted with or without DAPI. Staining was visualized with a Leica fluorescence microscope.

NICD Transcriptional Activity Assay

Fibroblasts were transiently cotransfected with 4XCBF-luciferase cDNA and empty vector (pCS2), myc-tagged mΔENotch-coding vectors, or NICD-coding vectors. A β-gal reporter cDNA was cotransfected to normalize data for transfection efficiency. Forty-eight hours after transfection, cells were rinsed, gently scraped in PBS (pH, 7.4), and spun for 5 min at 4000 rpm. Cells were then homogenized in 100 μl of lysis buffer, and luciferase activity was measured by the Luciferase Assay System as described (Petit et al., 2001).

Gel Shift Assay

Electrophoretic mobility shift assays (EMSA) were performed using a commercial DNA binding-protein detection system (Promega, Charbonnières, France). In brief, PCR fragments covering three distinct regions of the rNEPP1 promoter were obtained using the following primer pairs 5′AAGCTTGACCGAGAGC3′/5′CGACACATCC

CGACC3′ raising a 295 bp probe, 5′GGAACCTCCCCCAAGTCC3′/5′CCTTTCTCCCTCAGC3′ (219 bp probe), and 5′GGTCGGGATGTGTCG3′/5′CAGTAGCGGCTCCTTCC3′ (301 bp probe); then the fragments were end labeled using [^{32}P]ATP (6000 Ci/mmol, ICN Biomedicals, Orsay, France). For the preparation of nuclear extracts, HEK293 cells were cultivated in 100 mm diameter dishes and transiently transfected with 12 μg cDNA of either empty pcDNA3 vector or a mix of myc-tagged-AICDC59 (6 μg), TIP60 (3 μg), and Fe65 (3 μg) by means of DAC30 reactive as previously described. Forty-eight hours after transfection, cells were harvested and nuclear extracts were prepared according to the *Current Protocols in Molecular Biology* (Ausubel et al., 2002). Binding reactions containing nuclear extracts (10 μg) were performed at 37°C, using the shorter 219 bp probe according to the manufacturer's directions. Then protein-DNA complexes were resolved by electrophoresis through 7% native polyacrylamide gels in buffer containing 5mM Tris (pH, 8.3) and 38 mM Glycine for 3 hr at 300V. Gels were dried and autoradiographed on a BAS-1500 phosphorimager (Fujifilm, Tokyo, Japan). The specificity of the above described reactions were verified by Supershift gel assay corresponding to the preincubation of nuclear extracts with either anti-myc (specific) or anti-rabbit (nonspecific) antibodies before allowing the binding reactions and subsequent incorporation of the labeled probe.

Normal and Pathological Human Brain Tissues

All brain samples correspond to frontal cortices. Samples from Rouen include a control brain (female, 74 years) and one Familial AD brain (female, 51 years, Leu392Val-PS1 mutation). Samples from la Pitié Salpêtrière (Paris) correspond to two control brains (males, 72 and 55 years), two sporadic AD brains (females, 75 and 82 years), and two Familial AD brains (female, 37 years, Leu235Pro-PS1 mutation; male, 44 years, Phe386Ser-PS1 mutation).

Statistical Analysis

Statistical analyses were performed with PRISM Software (GraphPad Software, San Diego) by using the unpaired Student's t test for pairwise comparisons.

Acknowledgments

We sincerely thank Drs. B. De Strooper, P. Saftig, F. Chen, Q. Hu, G. Martin, C. Dumanchin, D. Campion, N. Girardot, and C. Duyckaerts for providing cell lines and brain tissues. We are grateful to Drs. T.C. Sudhof, R. Kopan, P. Marambaud, J.P. Borg, F. Authier, G. Boileau, L. Mercken, and W. Araki for generously providing us with cDNAs and antibodies. This work was supported by the EU contract LSHM-CT-2003-503330 (APOPIS), by the Association France Alzheimer (RPP) and by the Fondation pour la Recherche Médicale (C.S.). Drs. P. St. George-Hyslop and Toshitaka Kawarai are supported by the Canadian Institutes of Health Research, Howard Hughes Medical Institute, and Alzheimer Society of Ontario. This work is dedicated to our friend and colleague Nicole Boyer, who died suddenly on April 19, 2005.

Received: August 24, 2004
Revised: November 17, 2004
Accepted: April 12, 2005
Published: May 18, 2005

References

Alves da Costa, C., Paitel, E., Mattson, M.P., Amson, R., Telerman, A., Ancolio, K., and Checler, F. (2002). Wild-type and mutated presenilin-2 trigger p53-dependent apoptosis and down-regulate presenilin-1 expression in HEK293 human cells and in murine neurons. Proc. Natl. Acad. Sci. USA *99*, 4043–4048.

Armogida, M., Petit, A., Vincent, B., Scarzello, S., Alves da Costa, C., and Checler, F. (2001). Endogenous β-amyloid production in presenilin-deficient embryonic mouse fibroblasts. Nat. Cell Biol. *3*, 1030–1033.

Ausubel, F.M., Brent, R., Kingston, R.E., Moore, D.D., Seidman, J.G., Smith, J.A., and Struhl, K. (2002). DNA-protein interactions. In Short Protocols in Molecular Biology, Fifth Edition, Vol. 2 (Boston: John Wiley and Sons), pp. 12.1.1–12.1.3.

Borg, J.-P., Yang, Y., De Taddeo-Borg, M., Margolis, B., and Turner, R.S. (1998). The X11α protein slows cellular amyloid precursor protein processing and reduces Aβ40 and Aβ42 secretion. J. Biol. Chem. *273*, 14761–14766.

Burdick, D., Soreghan, B., Kwon, M., Kosmoski, J., Knauer, M., Henschen, A., Yates, J., Cotman, C., and Glabe, C. (1992). Assembly and aggregation properties of synthetic Alzheimer's A4/beta amyloid peptide analogs. J. Biol. Chem. *267*, 546–554.

Cao, X., and Südhof, T.C. (2001). A transcriptively active complex of APP with Fe65 and histone acetyltransferase tip60. Science *293*, 115–120.

Carson, J.A., and Turner, A.J. (2002). β-amyloid catabolism: roles for neprilysin (NEP) and other metallopeptidases. J. Neurochem. *81*, 1–8.

Checler, F. (1993). Neuropeptide-degrading peptidases. In Methods in Neurotransmitters and Neuropeptides Research. Part 2., T. Nagatsu, H. Parvez, M. Naoi, and S. Parvez, eds. (Amsterdam: Elsevier Science Publishers), pp. 375–418.

Checler, F. (1999). Presenilins: Structural aspects and post-translational events. Mol. Neurobiol. *19*, 255–265.

Chen, F., Gu, Y., Hasegawa, H., Ruan, X., Arawaka, S., Fraser, P., Westaway, D., Mount, H., and St. George-Hyslop, P. (2002). Presenilin 1 mutations activate γ-42-secretase but reciprocally inhibit ε-secretase cleavage of APP and S3-cleavage of Notch. J. Biol. Chem. *277*, 36521–36526.

De Strooper, B. (2003). Aph-1, Pen-2, and nicastrin with presenilin generate an active γ-secretase complex. Neuron *38*, 9–12.

De Strooper, B., Saftig, P., Craessaerts, K., Vanderstichele, H., Guhde, G., Von Figura, K., and Van Leuven, F. (1998). Deficiency of presenilin 1 inhibits the normal cleavage of amyloid precursor protein. Nature *391*, 387–390.

De Strooper, B., Annaert, W., Cupers, P., Saftig, P., Craessaerts, K., Mumm, J.S., Schroeter, E.H., Schrijvers, V., Wolfe, M.S., Ray, W.J., et al. (1999). A presenilin-1-dependent γ-secretase-like protease mediates release of Notch intracellular domain. Nature *398*, 518–522.

Dovey, H.F., John, V., Anderson, J.P., Chen, L.Z., de Saint Andrieu, P., Fang, L.Y., Freedman, S.B., Folmer, B., Goldbach, E., Holsztynska, E.J., et al. (2001). Functional gamma-secretase inhibitors reduce beta-amyloid peptide levels in brain. J. Neurochem. *76*, 173–181.

Eckman, E.A., Watson, M., Marlow, L., Sambamurti, K., and Eckman, C.B. (2003). Alzheimer's disease β-amyloid peptide is increased in mice deficient in endothelin-converting enzyme. J. Biol. Chem. *278*, 2081–2084.

Farris, W., Mansourian, S., Chang, Y., Lindsley, L., Eckman, E.A., Frosch, M.P., Eckman, C.B., Tanzi, R.E., Selkoe, D.J., and Guénette, S. (2003). Insulin-degrading enzyme regulates the levels of insulin, amyloid β-protein, and the β-amyloid precursor protein intracellular domain in vivo. Proc. Natl. Acad. Sci. USA *100*, 4162–4167.

Francis, R., McGrath, G., Zhang, J., Ruddy, D.A., Sym, M., Apfeld, J., Nicoll, M., Maxwell, M., Hai, B., Ellis, M.C., et al. (2002). *aph-1* and *pen-2* are required for notch pathway signaling, γ-secretase cleavage of βAPP, and presenilin protein accumulation. Dev. Cell *3*, 85–97.

Gu, Y., Misonou, H., Sato, T., Dohmae, N., Takio, K., and Ihara, Y. (2001). Distinct intramembrane cleavages of the β-amyloid precursor protein family resembling γ-secretase-like cleavage of Notch. J. Biol. Chem. *276*, 35235–35238.

Haass, C., and De Strooper, B. (1999). The presenilins in Alzheimer's disease—proteolysis holds the key. Science *286*, 916–919.

Haass, C., and Selkoe, D.J. (1993). Cellular processing of β-amyloid precursor protein and the genesis of amyloid β-peptide. Cell *75*, 1039–1042.

Hama, E., Shirotani, K., Masumoto, H., Sekine-Aizawa, Y., Aizawa, H., and Saido, T.C. (2001). Clearance of extracellular and cell-asso-

ciated amyloid β peptide through viral expression of neprilysin in primary neurons. J. Biochem. (Tokyo) *130*, 721–726.

Hauss-Wegrzyniak, B., and Wenk, G.L. (2002). Beta-amyloid deposition in the brains of rats chronically infused with thiorphan or lipopolysaccharide: the role of ascorbic acid in the vehicle. Neurosci. Lett. *322*, 75–78.

Heber, S., Herms, J., Gajic, V., Hainfellner, J.A., Aguzzi, A., Rülicke, T., Kretzschmar, H., von Koch, C., Sisodia, S.S., Tremml, P., et al. (2000). Mice with combined gene knock-outs reveal essential and partially redundant functions of amyloid precursor protein family members. J. Neurosci. *20*, 7951–7963.

Herreman, A., Hartmann, D., Annaert, W., Saftig, P., Craessaerts, K., Serneels, L., Umans, L., Schrijvers, V., Checler, F., Vanderstichele, H., et al. (1999). Presenilin 2 deficiency causes a mild pulmonary phenotype and no changes in amyloid precursor protein processing but enhances the embryonic lethal phenotype of presenilin 1 deficiency. Proc. Natl. Acad. Sci. USA *96*, 11872–11877.

Herreman, A., Serneels, L., Annaert, W., Collen, D., Schoonjans, L., and De Strooper, B. (2000). Total inactivation of γ-secretase activity in presenilin-deficient embryonic stem cells. Nat. Cell Biol. *2*, 461–462.

Ishimaru, F., Mari, B., and Shipp, M.A. (1997). The type 2 CD10/neutral endopeptidase 24.11 promoter: functional characterization and tissue-specific regulation by CBF/NF-Y isoforms. Blood *89*, 4136–4145.

Iwata, N., Tsubuki, S., Takaki, Y., Shirotani, K., Lu, B., Gerard, N.P., Gerard, C., Hama, E., Lee, H.-J., and Saido, T.C. (2001). Metabolic regulation of brain Aβ by neprilysin. Science *292*, 1550–1552.

Kimberly, W.T., Zheng, J.B., Guénette, S., and Selkoe, D.J. (2001). The intracellular domain of the β-amyloid precursor protein is stabilized by Fe65 and translocates to the nucleus in a Notch-like manner. J. Biol. Chem. *276*, 40288–40292.

King, G.D., and Turner, R.S. (2004). Adaptor protein interactions: modulators of amyloid precursor protein metabolism and Alzheimer's disease risk? Exp. Neurol. *185*, 208–219.

Kinoshita, A., Whelan, C.M., Smith, C.J., Berezovska, O., and Hyman, B.T. (2002). Direct visualization of the gamma secretase-generated carboxy-terminal domain of the amyloid precursor protein: association with Fe65 and translocation to the nucleus. J. Neurochem. *82*, 839–847.

Kopan, R., and Goate, A. (2000). A common enzyme connects Notch signaling and Alzheimer's disease. Genes Dev. *14*, 2799–2806.

Kopan, R., Schroeter, E.H., Weintraub, H., and Nye, J.S. (1996). Signal transduction by activated mNotch: importance of proteolytic processing and its regulation by the extracellular domain. Proc. Natl. Acad. Sci. USA *93*, 1683–1688.

Lee, J.-H., Lau, K.-F., Perkinton, M.S., Standen, C.L., Shemilt, S.J.A., Mercken, L., Cooper, J.D., McLoughlin, D.M., and Miller, C.C.J. (2003). The neuronal adaptor protein X11α reduces Aβ levels in the brains of Alzheimer's APPswe Tg2576 transgenic mice. J. Biol. Chem. *278*, 47025–47029.

Leissring, M.A., Murphy, M.P., Mead, T.R., Akbari, Y., Sugarman, M.C., Jannatipour, M., Anliker, B., Müller, U., Saftig, P., de Strooper, B., et al. (2002). A physiologic signaling role for the γ-secretase-derived intracellular fragment of APP. Proc. Natl. Acad. Sci. USA *99*, 4697–4702.

Leissring, M.A., Farris, W., Chang, A.Y., Walsh, D.M., Wu, X., Sun, X., Frosch, M.P., and Selkoe, D.J. (2003). Enhanced proteolysis of β-amyloid in APP transgenic mice prevents plaque formation, secondary pathology and premature death. Neuron *40*, 1087–1093.

Luo, W.J., Wang, H., Li, H., Kim, B.S., Shah, S., Lee, H.-J., Thinakaran, G., Kim, T.-W., Yu, G., and Xu, H. (2003). PEN-2 and APH-1 coordinately regulate proteolytic processing of presenilin 1. J. Biol. Chem. *278*, 7850–7854.

Marambaud, P., Shioi, J., Serban, G., Georgakopoulos, A., Sarner, S., Nagy, V., Baki, L., Wen, P., Efthimiopoulos, S., Shao, Z., et al. (2002). A presenilin-1/γ-secretase cleavage releases the E-cadherin intracellular domain and regulates disassembly of adherens junctions. EMBO J. *21*, 1948–1956.

Marambaud, P., Wen, P.H., Dutt, A., Takashima, A., Siman, R., and Robakis, N. (2003). A CPB binding transcriptional repressor produced by the PS1/ε-cleavage of N-cadherin is inhibited by PS1 FAD mutations. Cell *114*, 635–645.

Marr, R.A., Rockenstein, E., Mukherjee, A., Kindy, M.S., Hersh, L.B., Gage, F.H., Verma, I.M., and Masliah, E. (2003). Neprilysin gene transfer reduces human amyloid pathology in transgenic mice. J. Neurosci. *23*, 1992–1996.

Paitel, E., Sunyach, C., Alves da Costa, C., Bourdon, J.C., Vincent, B., and Checler, F. (2004). Primary cultured neurons devoid of cellular prion display lower responsiveness to staurosporine through the control of p53 at both transcriptional and post-transcriptional levels. J. Biol. Chem. *279*, 612–618.

Passer, B., Pellegrini, L., Russo, C., Siegel, R.M., Lenardo, M.J., Schettini, G, Bachmann, M., Tabaton, M., and D'Adamio, L. (2000). Generation of an apoptotic intracellular peptide by γ-secretase cleavage of Alzheimer's amyloid β protein precursor. J. Alzheimers Dis. *2*, 289–301.

Petit, A., Bihel, F., Alves da Costa, C., Pourquié, O., Kraus, J.L., and Checler, F. (2001). New protease inhibitors prevent γ-secretase-mediated Aβ 40/42 production without affecting Notch cleavage. Nat. Cell Biol. *3*, 507–511.

Pollack, S.J., and Lewis, H. (2005). γ-secretase inhibitors for Alzheimer's disease: challenges of a promiscuous protease.. Curr. Opin. Investig. Drugs *6*, 35–47.

Roques, B.P., Noble, F., Dauge, V., Fournie-Zaluski, M.C., and Beaumont, A. (1993). Neutral endopeptidase 24.11: structure, inhibition and experimental and clinical pharmacology. Pharmacol. Rev. *45*, 87–146.

Sastre, M., Turner, R.S., and Levy, E. (1998). X11 interaction with β-amyloid precursor protein modulates its cellular stabilization and reduces amyloid β-protein secretion. J. Biol. Chem. *273*, 22351–22357.

Sastre, M., Steiner, H., Fuchs, K., Capell, A., Multhaup, G., Condron, M.M., Teplow, D.B., and Haass, C. (2001). Presenilin dependent γ-secretase processing of β-amyloid precursor protein at a site corresponding to the S3 cleavage of Notch. EMBO Rep. *2*, 835–841.

Saura, C.A., Choi, S.-Y., Beglopoulos, V., Malkani, S., Zhang, D., Rao, B.S.S., Chattarji, S., Kelleher, R.J. III, Kandel, E.R., et al. (2004). Loss of presenilin function causes impairments of memory and synaptic plasticity followed by age-dependent neurodegeneration. Neuron *42*, 23–36.

Shearman, M.S., Beher, D., Clarke, E.E., Lewis, H.D., Harrison, T., Hunt, P., Nadin, A., Smith, A.L., Stevenson, G., and Castro, J.L. (2000). L-685,458, an aspartyl protease transition state mimic, is a potent inhibitor of amyloid β-protein precursor γ-secretase activity. Biochemistry *39*, 8698–8704.

Shen, J., Bronson, R.T., Chen, D.F., Xia, W., Selkoe, D., and Tonegawa, S. (1997). Skeletal and CNS defects in presenilin-1-deficient mice. Cell *89*, 629–639.

Shirotani, K., Tsubuki, S., Iwata, N., Takaki, Y., Harigaya, W., Maruyama, K., Kiryu-Seo, S., Kiyama, H., Iwata, H., Tomita, T., et al. (2001). Neprilysin degrades both amyloid β peptides 1–40 and 1–42 most rapidly and efficiently among thiorphan- and phosphoramidon-sensitive endopeptidases. J. Biol. Chem. *276*, 21895–21901.

Sisodia, S.S., and St. George-Hyslop, P. (2002). γ-secretase, Notch, Aβ and Alzheimer's disease: where do presenilins fit in? Nat. Rev. Neurosci. *3*, 281–290.

Suda, H., Aoyagi, T., Takeuchi, T., and Umezawa, H. (1973). Letter: A thermolysin inhibitor produced by actinomycetes: phosphoramidon. J. Antibiot. (Tokyo) *26*, 621–623.

Vassar, R., and Citron, M. (2000). Aβ-generating enzymes: recent advances in β- and γ-secretases research. Neuron *27*, 419–422.

Vincent, B., Beaudet, A., Dauch, P., Vincent, J.P., and Checler, F. (1996). Distinct properties of neuronal and astrocytic endopeptidase 3.4.24.16: a study on differentiation, subcellular distribution and secretion processes. J. Neurosci. *16*, 5049–5059.

Wang, B., Hu, Q., Hearn, M.G., Shimizu, K., Ware, C.B., Liggitt, D.H.,

Jin, L.-W., Cool, B.H., Storm, D.R., and Martin, G.M. (2004). Isoform-specific knockout of *Fe65* leads to impaired learning and memory. J. Neurosci. Res. *75*, 12–24.

Weidemann, A., Eggert, S., Reinhard, F.B.M., Vogel, M., Paliga, K., Baier, G., Masters, C.L., Beyreuther, K., and Evin, G. (2002). A novel ε-cleavage within the transmembrane domain of the Alzheimer amyloid precursor protein demonstrates homology with the Notch processing. Biochemistry *41*, 2825–2835.

Wolfe, M.S., Citron, M., Diehl, T.S., Xia, W., Donkor, I.O., and Selkoe, D.J. (1998). A substrate-based difluoro ketone selectively inhibits Alzheimer's γ-secretase activity. J. Med. Chem. *41*, 6–9.

Wolfe, M.S., Xia, W., Ostaszewski, B.L., Diehl, T.S., Kimberly, W.T., and Selkoe, D.J. (1999). Two transmembrane aspartates in presenilin-1 required for presenilin endoproteolysis and γ-secretase activity. Nature *398*, 513–517.

Yu, G., Nishimura, M., Arawaka, S., Levitan, D., Zhang, L., Tandon, A., Song, Y.-Q., Rogaeva, E., Chen, F., Kawarai, T., et al. (2000). Nicastrin modulates presenilin-mediated *notch/glp1* signal transduction and βAPP processing. Nature *407*, 48–54.

Zhang, Z., Nadeau, P., Song, W., Donoviel, D., Yuan, M., Bernstein, A., and Yankner, B.A. (2000). Presenilins are required for γ-secretase cleavage of βAPP and transmembrane cleavage of Notch. Nat. Cell Biol. *2*, 463–465.